

Current issue list available at Ann Med Res

# Annals of Medical Research

journal page: annalsmedres.org



# Diagnostic performance of simplified intravoxel incoherent motion DWI for breast lesions

Serap Karabiyik <sup>a, o, \*</sup>, Saime Ramadan <sup>b, o</sup>, Emil Settarzade <sup>c, o</sup>, Ali Ilker Filiz <sup>d, o</sup>, Hatice Ozturkmen Akay <sup>e, o</sup>

#### MAIN POINTS

## This study evaluated the diagnostic utility of simplified IVIM (SI-IVIM) with three b-values in distinguishing malignant from benign breast lesions, showing comparable but not superior accuracy to conventional ADC.

- Median and minimum perfusion fraction (f) values yielded the highest AUCs (0.79 and 0.76), indicating potential as supplementary markers when diffusion imaging results are inconclusive.
- Despite advantages like shorter scan time and lower complexity, SI-IVIM's clinical utility is limited due to variability in perfusion estimates, necessitating validation in larger, diverse populations.

Cite this article as: Karabiyik S, Ramadan S, Settarzade E, Filiz AI, Ozturkmen Akay H. Diagnostic performance of simplified intravoxel incoherent motion DWI for breast lesions. *Ann Med Res.* 2025;32(6):264–271. doi: 10.5455/annalsmedres.2024.12.259.

#### ■ ABSTRACT

**Aim:** To assess the success of 3*b*-value simplified intravoxel incoherent motion (SI-IVIM) diffusion-weighted imaging (DWI) in distinguishing malignant from benign breast lesions.

**Materials and Methods:** Sixty-four breast lesions in 59 women were retrospectively analyzed. Patients with MRI-negative lesions, lesions smaller than 8 mm, poor-quality DWI, or indeterminate lesions without surgical excision were excluded. All MRIs scans were conducted using a 1.5 T MRI scanner, including DWI (b values: 0, 100, 800, and 1500 s/mm²), and dynamic contrastenhanced sequences (DCE-MRI). Lesions were segmented manually using the ITKsnap program with the help of DCE-MRI, and volumetric mask images (VOI) were generated. Different apparent diffusion coefficient (ADC) values and IVIM parameters, D=ADC (100,1500) and f= f(0, 50, 800), were computed. The diagnostic performances of different ADC values and IVIM parameters were compared to define sensitivity, specificity and the optimal cut-off values.

**Results:** Maximum (max) ADC100, median (med) ADC800, med ADC1500, med f and minimum (min) f values showed significant differences between benign and malignant breast lesions. Med D and min D were lower in the malignant group; however, this difference did not reach statistical significance. The diagnostic performances of med f (AUC= 0.79) and min f (AUC= 0.76) were superior to those of the conventional ADC value (ADC800, AUC= 0.74) in the ROC curve analysis. However, in the DeLong test analysis, neither med f nor min f demonstrated statistically significant diagnostic superiority over the other parameters.

**Conclusion:** The SI-IVIM parameters showed no significant diagnostic superiority over the ADC value in differentiating malignant breast lesions.

**Keywords:** Breast neoplasms, Diffusion magnetic resonance imaging, Simplified IVIM, Intravoxel-incoherent motion

Received: Dec 28, 2024 Accepted: Jun 16, 2025 Available Online: Jun 25, 2025



Copyright © 2025 The author(s) - Available online at annalsmedres.org. This is an Open Access article distributed under the terms of Creative Commons Attribution-NonCommercial-NoDerivatives 4.0 International License.

#### **■ INTRODUCTION**

The most sensitive imaging method for breast cancer detection is dynamic contrast-enhanced magnetic resonance imaging (DCE-MRI) [1]. However, its specificity is generally less than 80% [2]. Advanced imaging techniques are crucial in the era of precision medicine, because they play a central role in directing therapeutic decisions, improving diagnos-

tic accuracy, and customizing treatment options. Diffusion-weighted imaging (DWI) has emerged as a promising noninvasive method for distinguishing between breast cancer and benign lesions, differentiating between in situ and invasive lesions, and predicting the efficacy of neoadjuvant therapy using apparent diffusion coefficient (ADC) values [3-6]. However, breast cancer typically exhibits a high number of cells

<sup>&</sup>lt;sup>a</sup>Istanbul Training and Research Hospital, Department of Radiology, Istanbul, Türkiye

<sup>&</sup>lt;sup>b</sup>Baskent University, Faculty of Medicine, Istanbul Hospital, Department of Pathology, Istanbul, Türkiye

<sup>&</sup>lt;sup>c</sup>Zollernalb Klinikum, Radiologie Abteilung, Radiology Section, Balingen, Germany

<sup>&</sup>lt;sup>d</sup>Baskent University, Faculty of Medicine, Istanbul Hospital, Department of General Surgery, Istanbul, Türkiye

<sup>&</sup>lt;sup>e</sup>Baskent University, Faculty of Medicine, Istanbul Hospital, Department of Radiology, Istanbul, Türkiye

<sup>\*</sup>Corresponding author: serapyucl@gmail.com (Serap Karabiyik)

(low diffusivity) and a high number of blood vessels (high perfusion), which may have opposite effects on ADC values [7]. Intravoxel incoherent motion (IVIM) MRI can reveal details regarding the diffusion and perfusion properties of tissues, particularly in the context of blood flow in the microvasculature, by using multi-b-value DWI [8, 9]. It provides separate measurements of pure diffusion (D), representing the mobility of water molecules in tissue; pseudodiffusion ( $D^*$ ), which depends on the length of the microvessel segments and blood velocity; and the microvascular volume fraction (f), which reflects the contribution of microvascular blood flow without the use of a contrast agent [7].

In the IVIM technique, nonlinear least-squares fitting procedures without any constraints are generally used. employed to determine the values of D,  $D^*$ , and f simultaneously. To utilize fitting algorithms, multiple DWI sequences with a wide range of b values are needed to be acquired, which leads to prolonged acquisition durations [10]. Furthermore, these methods frequently result in numerical instabilities, inadequate repeatability, and incorrect parameter values for  $D^*$ and f in tissues having low perfusion [11]. SI-IVIM operates under the assumption of the pseudodiffusion has diminished to zero in b values that exceed a sufficiently large threshold, which may overcome the instability of the multi-b value IVIM. To achieve SI-IVIM analysis, acquiring DWI sequences with three or four distinct b values is necessary [12]. SI-IVIM offers reduced computational complexity and faster data analysis, which benefits clinical settings by improving patient comfort and compliance through quicker data acquisition [13]. However, simplified models may compromise accuracy and reliability in parameter estimation by overlooking complex tissue interactions, leading to variability and reduced precision in distinguishing tissue types or pathologies.

Few studies have investigated the efficacy of SI-IVIM in distinguishing between malignant and benign breast lesions [13, 14]. To address this problem, the primary objective of this study was to assess SI-IVIM to distinguish malignant from benign breast lesions.

#### ■ MATERIALS AND METHODS

#### Patient population

This retrospective study was approved by the local institutional review board (Protocol no: KA23/73). The requirement for informed patient consent was waived because of the retrospective nature of the study. We retrospectively reviewed patients between April 2021 and March 2023 who have suspicious breast lesions on ultrasound, mammography or MRI and had biopsy (ACR BI-RADS scores of 4 or 5 breast lesions). The primary indications for breast MRI encompassed preoperative staging, surveillance of high-risk patient populations, and the assessment of indeterminate findings detected on mammography or ultrasound. Patients with MRI-negative lesions, lesions smaller than 8 mm to prevent the influence of partial volume effects, low DWI quality, and lesions

with unknown malignant potential (papillary lesions, flat epithelial atypia, lobular neoplasia, atypical ductal hyperplasia, radial scar) without surgical excision were excluded from patient population of the study (Figure 1). A total of 64 breast lesions in 59 women (five patients with 2 suspicious breast lesions), with ages between 24 to 99 years and a mean age of 53.38±15.17 years, were included in the study.

# MRI data acquisition and DWI parameters

All MRIs were conducted with the patient lying face down using a breast coil with four channels with a 1.5 T MRI scanner (MAGNETOM Avanto, Siemens Healthcare, Erlangen, Germany). The following sequences were acquired as part of the routine clinical protocol: axial turbo spin-echo (TSE) T1, axial turbo inversion recovery magnitude (TIRM), axial spin-echo echo-planar imaging (EPI), and dynamic contrastenhanced magnetic resonance imaging (DCE-MRI) using a 3D fat-saturated gradient echo axial sequence (TR/TE: 4.60/1.42 ms; flip angle: 6°; NEX: 1 slice thickness:1 mm; matrix size:  $358 \times 448$ ; FOV:  $340 \times 100$ ), six phases after injection of intravenous 0.2 mL/kg gadoterate meglumine (Dotarem). Four b-values (0, 100, 800, and 1500 s/mm<sup>2</sup>) in three orthogonal orientations were obtained for an EPI sequence using fat suppression (SPAIR) with the following parameters: acquisition time of 6.5 minutes, TR/TE of 7400/78 ms, matrix size of  $63 \times 164$ , FOV of  $340 \times 390$  mm, slice thickness of 4 mm, slice gap of 4 mm, and NEX of 5.

### Postprocessing and Image analysis

In previous research, the IVIM method employed the following equation to calculate its parameters in a streamlined manner [12, 13, 15].

$$ADC(i,j) = \frac{ln(S(b_i)) - ln(S(b_j))}{j - i}$$

Utilizing this specified equation, the different ADC values were calculated.

D and f were estimated using the method proposed by Le Bihan [15]. Previous studies have suggested that b-values > 200 s/mm<sup>2</sup> should be used to minimize the influence of perfusion effects [11]. Based on this information, we calculated the f values using b-values of b0=0,  $b_1$ =800, and  $b_2$ =1500 s/mm<sup>2</sup>.

$$D = ADC(100, 1500) = \frac{ln(S(b_1)) - ln(S(b_2))}{b2 - b1}$$
  
$$f = f(0.800, 1500) = 1 - \frac{S(b_2)}{S(0)} \cdot exp^{D \cdot b_2}$$

### Volume of interest (VOI)

DWI images were registered with post-contrast images using ITK-SNAP (http://www.itksnap.org) software. A proficient breast radiologist with four years of expertise in breast radiology manually delineated the lesions seen on the post-contrast second phase of DCE-MRI scans (Figure 2). The segmentation process involved outlining the outer boundary of the tumor on each image slice, while excluding areas of hemorrhage, necrosis, or cystic elements. In cases of multifocal or



Figure 1. Flow chart of study population.



**Figure 2.** Segmentation of the mass and the contralateral normal breast tissue. An irregular contoured mass with invasive ductal carcinoma diagnosis in the outer-lower quadrant of the right breast is visible in the contrast-enhanced axial image (A) and the b = 0 DWI map (B). The segmentation of the mass (outlined with white line) and the contralateral normal breast (outlined with dashed white line) in the b = 0 DWI sequence which is used to create the mask image is seen (C). The contralateral normal breast was segmented ensure a volume comparable to the mass lesion.

multicentric tumors, only the primary lesion with the largest size was segmented. Volumetric mask images were generated for both lesions and normal fibroglandular structures of the contralateral breast using the VOI method based on DCE images and b=0 images in the ITKsnap. Following visual confirmation to ensure correct anatomical alignment between DCE images and images with varying b values, the VOI was transferred to the parameter maps. Subsequently, the average intensity values of the various ADC values, D, and f, were automatically computed from the mask images using the fslstats command.

# Statistical analysis

Statistical analyses were performed using IBM SPSS Statistics for Windows, Version 22.0 (Armonk, NY: IBM Corp.) and R Studio (version 2023.06.1+524; Posit, PBC, Boston, MA, USA). Post-test power analysis was performed using Cohen's d effect size calculations and two-sided t-tests with  $\alpha$ =0.05 to evaluate the achieved statistical power for each radiological parameter. Continuous data are presented as mean standard deviation or median and interquartile range (IQR, 25-75th percentile). Kolmogorov-Smirnov (K-S) test was used to analyze the normal distribution assumption of the quantitative outcomes. The student's t-test was used to compare normally distributed variables, while the Mann-Whitney U test was applied for non-normally distributed variables. The Delong test was used to compare area under the curve (AUC) values to investigate whether any parameter exhibited diagnostic superiority. The diagnostic performance of different IVIM parameters was evaluated using receiver operating characteristic (ROC) curve analysis. The optimal cut-off values, for the parameters that showed statistically significant differences, in the ROC analysis were determined using the Youden Index, which maximizes the sum of sensitivity and specificity to achieve the best diagnostic threshold. For each parameter, the sensitivity and specificity were calculated along with their 95% confidence intervals (CI). Differences in IVIM parameters among different immunohistochemical subtypes were analyzed using the Kruskal-Wallis test for non-normally distributed variables and one-way ANOVA for normally distributed variables. Correlations between IVIM parameters and tumor immunohistochemical features were assessed using the Pearson correlation coefficient (r) for normally distributed data and the Spearman correlation coefficient ( $\rho$ ) for non-normally distributed data. A p-value < 0.05 was considered statistically significant.

#### **■ RESULTS**

A total of 64 breast lesions were analyzed, comprising 35 (54.7%) malignant and 29 (45.3%) benign lesions. The descriptive statistics of the lesions are presented in Table 1.

Several parameters showed statistically significant differences between the malignant and benign groups (Figure 3). Among these, the median (med) f and minimum (min) f had the lowest p-values (p< 0.001) (Table 2).

Med D and min D were lower in the malignant group, but this difference was not significant (p= 0.184 and p= 0.210, respectively).

The diagnostic performances of med f (AUC= 0.79) and min f (AUC= 0.76) were superior to that of the conventional

Table 1. Demographics of the patients and lesion characteristics.

	Malignant lesions	Benign lesions		
Breast side (% in columns)				
Right	24 (68.6)	18 (62.1)		
Left	11 (31.4)	11 (37.9)		
Mean age of the patient	58.37±14.88	47.34±13.42		
an diameter (mm) $28.26\pm15.93$		$14.38 \pm 6.40$		
(min-max)	(9-80)	(8-33)		
Mean volume(cm <sup>3</sup> )	$5.92{\pm}6.98$	$0.616 \pm 1.18$		
(min-max)	(0.20-30.21)	(0.05-6.51)		
Shape (% in columns)				
Mass	31 (88.6)	23 (79.3)		
Non-mass	4 (11.4)	6 (20.7)		
Histopathological subtype (% in columns)	Invasive carcinoma of no special type (NOS) 21 (60)	Fibroadenoma 12 (41.4)		
	Invasive lobular carcinoma (ILC) 4 (11.4)	Fibrocystic changes 10 (34.5)		
	Mixed IDC/ILC 2 (5.7)	Apocrine metaplasia 1 (3.4)		
	Mucinous carcinoma 1 (2.9)	Florid ductal hyperplasia 1 (3.4)		
	Tubular carcinoma 1 (2.9)	Mastitis 3 (10.3)		
	Mucoepidermoid carcinoma 1 (2.9)	Papilloma 2 (6.9)		
	Ductal carcinoma in situ 4 (11.4)			
	Focal microinvasive carcinoma on a background of papillary DCIS1 (2.9)			
Grade (% in columns)		-		
1	3 (8.6)			
2	15 (42.9)			
3	12 (34.3)			
HER-2 status (% in columns)		-		
Positive	5 (14.3)			
Negative	26 (74.3)			
Hormone receptor status (% in columns)				
Positive	31 (100)			
Negative	0 (0)	-		
Number of lesions (% in columns)				
Multifocal	10 (28.6)			
Multicentric	4 (11.4)	-		
One mass	14 (40)			
Immunohistochemical subtypes (% in columns)				
Luminal A	9 (25.7)			
Luminal B	17 (48.6)			
HER-2 positive	5 (14.3)			
Triple negative	0 (0)			

ADC value (ADC800, AUC= 0.74) in the ROC curve analysis (Table 3) (Figure 4). However, in the DeLong test analysis, neither med f nor min f demonstrated statistically significant diagnostic superiority over the other parameters.

The optimal cutoff value for med f was  $304.28 \times 10^{-3} \, \mathrm{mm^2/s}$ , yielding a sensitivity of 86.2% and a specificity of 65.7%, with a positive predictive value (PPV) of 85.2% and a negative predictive value (NPV) of 67.6%. (95% CI 68-91%). For min f, the optimal cut-off value was  $65.78 \times 10^{-3} \, \mathrm{mm^2/s}$ , resulting in a sensitivity of 82.7% and a specificity of 57.1% with a PPV of 80% and an NPV of 61.5% (95% CI 64-88%). Similarly, for ADC800, the optimal cut-off value was  $1.3 \times 10^{-3} \, \mathrm{mm^2/s}$ , achieving a sensitivity of 65.5% and a specificity of 85.7%, with a PPV of 75.7% and an NPV of 74.1% (95% CI 60-88%). Min f, and med f among different immunohistochemical subtypes, no significant differences were found between the

groups. Upon evaluating the correlation of these values with the receptor status and Ki-67, a negative correlation was observed between min f and Ki-67 ( $r_s$  = -0.45, p = 0.012). No significant correlations were detected for any other parameters.

Post-test power analysis revealed strong statistical power (>0.80) for medianADC800 (power=0.88), median f (power=0.99), and min f (power=0.98). Moderate power was observed for medianADC1500 (power=0.71) and max-ADC100 (power=0.66). The remaining parameters showed lower statistical power (<0.60) (Figure 5).

# **■ DISCUSSION**

In this study, the diagnostic efficacy of SI-IVIM parameters using three different *b* values was assessed to distinguish malignant from benign breast lesions. Although the AUC value

Table 2. Comparison of IVIM parameters.

Parameter	Benign'	Malignant'	p value	
Med ADC100*	1.80 (0.44-3.46)	1.75 (0.96-2.55)	0.677	
Min ADC100 * 0.79 (0.06-3.18) 0.3		0.394 (0.008-1.56)	0.161	
		6.65 (2.05-6.84)	0.007	
Med ADC800 t	1.31 ±0.42	1.03±0.27	0.001	
Min ADC800 *	0.84 (0.008-1.72)	1.01 (0.21-1.56)	0.118	
Max ADC800 t	1.81±037	1.83±0.35	0.863	
Med ADC1500 t	1.02±0.36	0.83±0.23	0.018	
Min ADC1500 *	0.62(0.03-1.42)0.4	0.44 (0.03-0.95)	0.104	
Max ADC1500 t	$1.44 \pm 0.36$	1.43±0.33	0.919	
Med D *	0.61 (0.07-1.38)	0.57 (0.05-1.20)	0.184	
Min D *	0.29 (0.002-1.09)	0.20 (0.004-0.63)	0.210	
lax D t 1.1±0.39		1.09±0.31	0.911	
Med f *	386.34 (157.60-586.99)	280.37 (155.16-457.98)	< 0.001	
Min f *	193.08 (13.25-488.87)	55.63 (4.03-260.87)	< 0.001	
Max f * 521.58 (336.49-790.12)		560.87 (396.87-717.75)	0.240	

Med: median, min: minimum, max: maximum. 'ADC, D, f values are given in units of  $10^{-3}$  mm<sup>2</sup>/s.\*:median(min-max) value and p value of Mann–Whitney U test, t: mean SD and p value of Student's t-test.

Table 3. ROC curve analysis.

Test Variables	AUC	Std. Error <sup>a</sup>	P value	Lower Bound	Upper Bound
Med f	0.79	0.06	<0.001	0.68	0.91
Min f	0.76	0.06	<0.001	0.64	0.88
Med ADC800	0.74	0.07	0.001	0.60	0.88
Max ADC100	0.70	0.07	0.010	0.56	0.83
Med ADC1500	0.70	0.07	0.005	0.57	0.84

of med f (AUC=0.79) and min f (AUC=0.76) were superior to that of the conventional ADC (ADC800 AUC=0.74), this difference was not statistically significant in the Delong test. Therefore, simplified IVIM with a 3-b value did not show diagnostic superiority to the ADC value in differentiating malignant breast lesions from benign ones.

This indicates that SI-IVIM could serve as a complementary imaging tool in breast lesion evaluation, potentially offering additional diagnostic insights in cases where conventional DWI findings are inconclusive. However, its clinical utility remains limited, and further studies with larger, more diverse patient populations are needed to validate its role in routine breast cancer assessment.

There are limited studies evaluating the diagnostic performance of simplified IVIM in breast lesions [13, 14]. Mürtz et al. studied the effectiveness of S-IVIM in the detection of breast lesions. They analyzed DWI data (b = 0, 50, 250, and 800 s/mm²) of 126 patients. They claimed that ADC, D1, and D2 were significantly smaller, and f1, f2, and  $D^*$  were significantly larger in malignant breast lesions than in benign lesions. Their findings also indicated that using DWI with b = 800 s/mm² as a standalone tool, the combination of D1+f1 achieved the highest discriminability with an accuracy of 93.7%, that was significantly higher than ADC at 86.9%, D1 alone at 88.0%, and f1 alone at 87.4%. When

DWI was used as adjunct to DCE-MRI, D1 (92.6%) showed the highest diagnostic accuracy as the single parameter, which was slightly, but not significantly, better than ADC (91.1%) and D2' (88.1%).

Li et al. compared the effectiveness of a 12-*b*-value traditional biexponential fitting model IVIM with a 3-*b*-value method in addition to DCE-MRI in 28 suspicious breast lesions. The study found that the 3-*b*-value method provided imaging parameters that were more accurate and had comparable or superior diagnostic values compared to traditional biexponential IVIM fitting [14].

In a meta-analysis by Arian et al. D and f values were significantly different between benign and malignant lesions, whereas  $D^*$  did not show any significant difference [16]. Malignant lesions had lower D and higher f values. MA et al. evaluated the diagnostic value of IVIM in breast lesions in a meta-analysis, they showed that D had the highest diagnostic performance with pooled sensitivity and specificity of 0.85 and 0.87, respectively [17]. Previous studies mostly showed lower D values and higher f values in malignant breast lesions than benign lesions [13, 18].

In our study, to eliminate the influence of perfusion in light of previous research, IVIM parameters were calculated using three values, specifically b values of 0, 800, and 1500 s/mm<sup>2</sup> [11]. Consequently, the  $D^*$  value could not be determined.

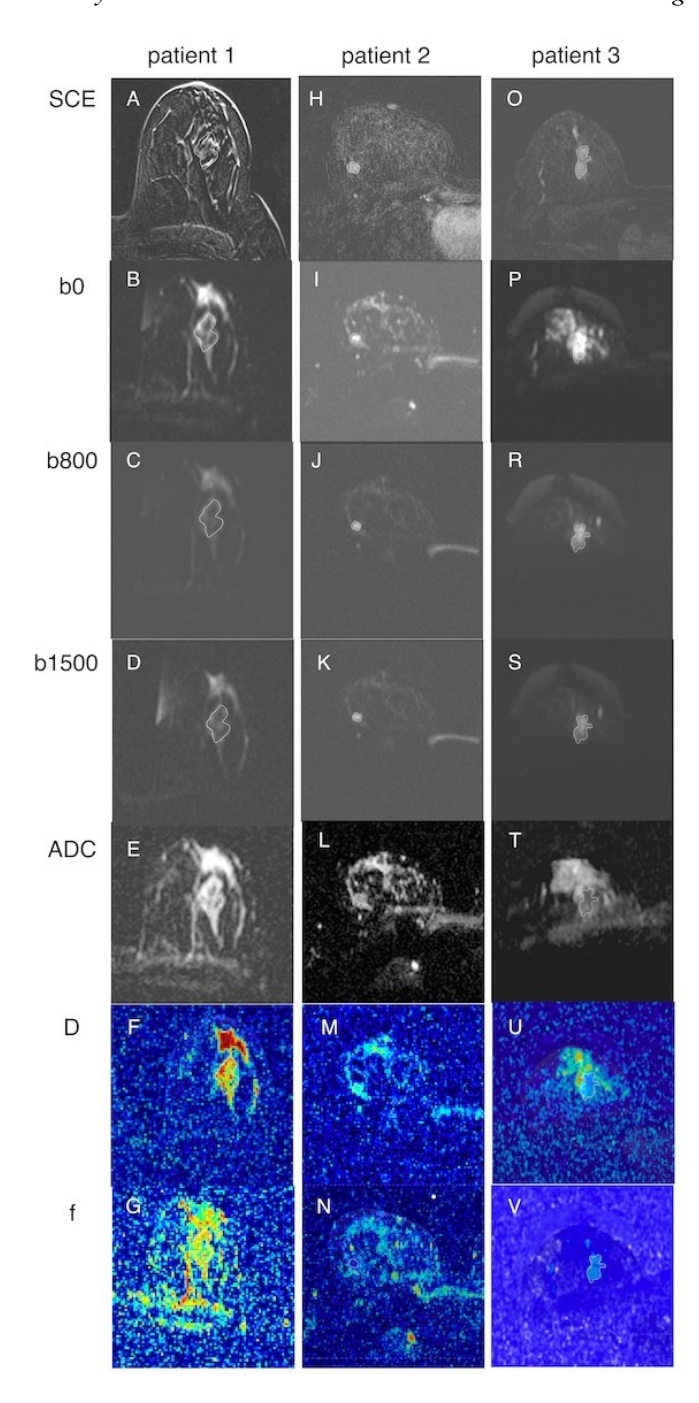


**Figure 3.** Axial MRI images of 3 different patients with following diagnosis: Lesion 1 (patient 1), fibroadenoma; lesion 2 (patient 2); invasive carcinoma of the no special type (grade 2 ER:60%, PR:55%, Her-2: negative, ki-67:40%); lesions 3 (patient 3), invasive lobular carcinoma (grade 2 ER, 95%; PR, 25%; Her-2, negative; ki-67:14%). First lesion appears with low signal intensity on the diffusion maps (C, D). It has high median ADC1500 (E, 1.21 x  $10^{-3}$  mm²/s), median D (F, 0.69 x  $10^{-3}$  mm²/s), and median f (G, 512.36 x  $10^{-3}$  mm²/s) values. Lesion 2 appeared hyperintense on diffusion maps (I, J). It has low median ADC1500 (L, 0.67 x  $10^{-3}$  mm²/s), median D (M, 0.55 x  $10^{-3}$  mm²/s), and f (N, 173.26 x  $10^{-3}$  mm²/s) values. Lesion 3 appeared hyperintense on the diffusion maps (R, S). It has low median ADC1500 (T, 0.79 x  $10^{-3}$  mm²/s), median D (U, 0.58 x  $10^{-3}$  mm²/s), and f (V, 131.18 x  $10^{-3}$  mm²/s) values.

The D values were lower in the malignant group, but this difference was not significant. Surprisingly, the med f and min f values were significantly lower in malignant lesions. Although

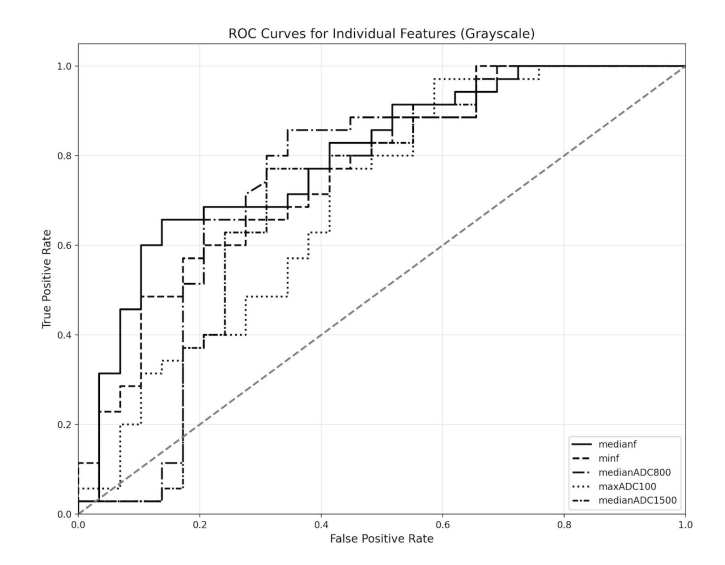


Figure 4. ROC curve analysis.

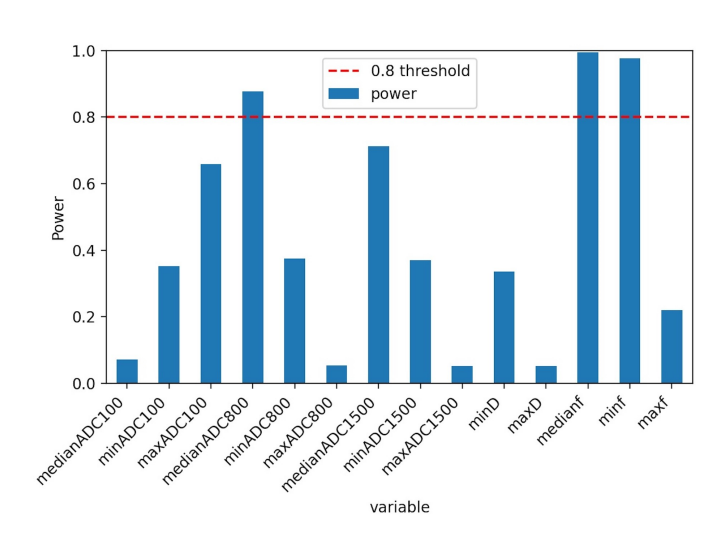


Figure 5. Post-test power analysis of IVIM parameters.

med f (AUC=0.79) showed a better diagnostic performance than conventional ADC (ADC800 AUC=0.74), this difference was not statistically significant. The reason for the reduced f can be explained by several factors. First, blood vessels in malignant tumors can be in abnormal structures that tend to be disorganized and leaky, so the overall blood flow within the tumor is lower than that in healthy tissue [19]. The dense cellular structure in malignant tumors may limit the movement of water molecules and the space available for blood perfusion, resulting in lower D and f values [11]. The heterogeneity of perfusion in breast tumors is a well-known issue. In one study, malignant lesions had an average of 27% of voxels with no perfusion at all [20]. Similarly, even more than 50% of the voxels exhibited no perfusion in another study [21]. Therefore, voxel-wise parameter calculations could be more accurate for perfusion analysis. Furthermore, unlike other simplified IVIM studies on the breast, the maximum b value in our study was b=1500, which is more susceptible to noise effects and Gaussian influences [22, 23]. Additionally, tumor

perfusion values represent a parameter that reflects tumor aggressiveness. In the present study, there were no cases of triplenegative breast tumors, and the number of HER-2-positive, which are characterized by aggressive immunohistochemical profiles, patients was limited. This may have contributed to the lower perfusion values [24].

Perucho et al. designed an IVIM study to optimize b values in patients with cervical cancer. They stated that, although three *b*-values were sufficient for a simplified model, *Dlinear* and *flinear* had error rates of 1% and 8%, respectively, failing to maintain discriminative capability [25].

Several studies have shown that DWI demonstrates significant diagnostic value in characterizing breast tumors and may offer higher specificity compared to traditional MRI techniques [17, 26]. DWI is performed with 2-b values and is based on the assumption of a mono-exponential fit to obtain a decay constant. However, the signal attenuation observed in monoexponential DWI is not always linear. DWI images fail to account for the microcirculation of blood. Le Bihan et al. introduced IVIM as a technique to differentiate the effects of diffusion and perfusion by applying a bi-exponential model to the signal decay using multiple b-values without requiring a contrast agent [15]. The traditional biexponential fitting model IVIM with multiple b values has some disadvantages, such as longer scanning time, increased complexity of execution and processing period, sensitivity to noise, and patient compliance [12]. SI-IVIM offers several advantages, such as reduced computational complexity and quicker and more straightforward data analysis, which are particularly advantageous in the clinical setting. Furthermore, the reduced time required to acquire data enhances patient comfort and compliance, which are essential considerations for regular clinical applications [13]. However, these methods have some disadvantages. An important drawback is the possible loss of accuracy and reliability in parameter estimation, because simplified models generally neglect the complex interactions between diffusion and perfusion within tissues. This may result in variability of parameters and decreased accuracy in differentiating tissue types or pathologies [27]. In IVIM imaging, the use of varying bvalue ranges leads to inconsistencies in the IVIM parameters. There is no established consensus on the optimal b values, which may lead to variability in the results. Perfusion effects are generally more pronounced at b-values below 200 s/mm<sup>2</sup>, and different thresholds can significantly alter IVIM parameters. Additional challenges, lack of standardized acquisition protocols, and different algorithms for analysis and motion artifacts, further affect the reliability and reproducibility of IVIM measurements [26, 28].

#### Limitations

The primary limitations of this study were the small number of patients and inadequate tumor diversity from an immunohistochemical perspective. Results of post-test power analysis suggests that larger sample sizes might be needed for more definitive conclusions about these metrics. Another limitation was that the segmentations were performed by a single individual, and neither the reproducibility of the VOIs nor the inter-observer variability was evaluated. In our study, a b-value of 1500 s/mm<sup>2</sup> was employed as the maximum b-value. This may result in higher non-Gaussian effects and noise-related biases [22, 23].

#### **■ CONCLUSION**

SI-IVIM parameters showed no significant diagnostic superiority over the ADC value in differentiating malignant breast lesions. Future studies conducted on larger and more diverse patient populations, as well as evaluating reproducibility and inter-observer variability, could further enhance the reliability and reproducibility of SI-IVIM for breast lesions.

**Ethics Committee Approval:** This study was approved by Baskent University Institutional Review Board and Ethics Committee (Protocol no: KA23/73).

**Informed Consent:** As the study was retrospective, the requirement for informed consent was waived.

Peer-review: Externally peer-reviewed.

**Conflict of Interest:** The authors declare that they have no known competing financial interests or personal relationships that could have appeared to influence the work reported in this paper.

**Author Contributions:** Conceptualization: SK; Supervision: HOA; Data curation: SK,SR, ES,AIF, HOA; Formal analysis: SK; Investigation: SK,SR, ES,AIF, HOA; Methodology: SK; Project administration: SK,SR, AIF, HOA; Resources: SK,SR, ES,AIF, HOA; Software: SK; Validation: SK; Visualization: SK; Writing-original draft: SK; Writing-review & editing: SK,SR, ES,AIF, HOA.

**Financial Disclosure:** This research did not receive any specific grant from funding agencies in the public, commercial, or not-for-profit sectors.

### **■ REFERENCES**

- Gilbert FJ, Pinker Domenig K. Diagnosis and staging of breast cancer: when and how to use mammography, tomosynthesis, ultrasound, contrast enhanced mammography, and magnetic resonance imaging.
   In: Diseases of the Chest, Breast, Heart and Vessels 2019 2022: *Diagnostic and Interventional Imaging*. 2019:155–66. DOI: 10.1007/978 3 030 11149 6\_13.
- Kuhl CK. Abbreviated magnetic resonance imaging (MRI) for breast cancer screening: rationale, concept, and transfer to clinical practice. *Annu Rev Med.* 2019;70:501–19. DOI: 10.1146/annurev med 121417 100403.
- Pinker K, Moy L, Sutton EJ, Mann RM, Weber M, Thakur SB, et al. Diffusion weighted imaging with apparent diffusion coefficient mapping for breast cancer detection as a stand alone parameter: comparison with dynamic contrast enhanced and multiparametric MRI. *Investig Radiol.* 2018;53(10):587–95. DOI: 10.1097/RLI.0000000000000465.

- Zhang L, Tang M, Min Z, Lu J, Lei X, Zhang X. Accuracy of combined dynamic contrast enhanced MRI and diffusion weighted imaging for breast cancer detection: a meta analysis. *Acta Radiol*. 2016;57(6):651–60. DOI: 10.1177/0284185115597265.
- Yu T, Li L, Shi J, Gong X, Cheng Y, Wang W, et al. Predicting histopathological types and molecular subtype of breast tumors: A comparative study using amide proton transfer weighted imaging, intravoxel incoherent motion and diffusion kurtosis imaging. *Magn Re*son Imaging. 2024;105:37–45. DOI: 10.1016/j.mri.2023.10.010.
- Baltzer P, Mann RM, Iima M, Sigmund EE, Clauser P, Gilbert FJ, et al. Diffusion weighted imaging of the breast—a consensus and mission statement from the EUSOBI International Breast Diffusion Weighted Imaging working group. Eur Radiol. 2020;30:1436–50. DOI: 10.1007/s00330-019-06510-3.
- 7. Liang J, Zeng S, Li Z, Kong Y, Meng T, Zhou C, et al. Intravoxel incoherent motion diffusion weighted imaging for quantitative differentiation of breast tumors: a meta analysis. *Front Oncol.* 2020;10:585486. DOI: 10.3389/fonc.2020.585486.
- 8. Le Bihan D, Breton E, Lallemand D, Grenier P, Cabanis E, Laval Jeantet M. MR imaging of intravoxel incoherent motions: application to diffusion and perfusion in neurologic disorders. *Radiology*. 1986;161(2):401-7. DOI: 10.1148/radiology.161.2.3763909.
- 9. Suo S, Cheng F, Cao M, Kang J, Wang M, Hua J, et al. Multiparametric diffusion weighted imaging in breast lesions: Association with pathologic diagnosis and prognostic factors. *J Magn Reson Imaging*. 2017;46(3):740–50. DOI: 10.1002/jmri.25612.
- While PT. Advanced methods for IVIM parameter estimation. In: Intravoxel Incoherent Motion (IVIM) MRI. *Jenny Stanford Publishing*; 2018. p. 449–84. DOI: 10.1201/9780429427275 23.
- 11. Liu C, Liang C, Liu Z, Zhang S, Huang B. Intravoxel incoherent motion (IVIM) in evaluation of breast lesions: comparison with conventional DWI. *Eur J Radiol.* 2013;82(12):e782–9. DOI: 10.1016/j.ejrad.2013.08.006.
- Mürtz P, Sprinkart A, Reick M, Pieper C, Schievelkamp A H, König R, et al. Accurate IVIM model based liver lesion characterisation can be achieved with only three b value DWI. Eur Radiol. 2018;28:4418–28. DOI: 10.1007/s00330-018-5401-7.
- 13. Mürtz P, Tsesarskiy M, Sprinkart AM, Block W, Savchenko O, Luetkens JA, et al. Simplified intravoxel incoherent motion DWI for differentiating malignant from benign breast lesions. *Eur Radiol Exp.* 2022;6(1):48. DOI: 10.1186/s41747-022-00298-6.
- 14. Li K, Machireddy A, Tudorica A, Moloney B, Oh KY, Jafarian N, et al. Discrimination of malignant and benign breast lesions using quantitative multiparametric MRI: a preliminary study. *Tomography*. 2020;6(2):148–59. DOI: 10.18383/j.tom.2019.00028.
- Le Bihan D, Breton E, Lallemand D, Aubin M L, Vignaud J, Laval Jeantet M. Separation of diffusion and perfusion in intravoxel incoherent motion MR imaging. *Radiology*. 1988;168(2):497–505. DOI: 10.1148/radiology.168.2.3393671.
- 16. Arian A, Seyed Kolbadi FZ, Yaghoobpoor S, Ghorani H, Saghazadeh A, Ghadimi DJ. Diagnostic accuracy of intravoxel incoherent motion (IVIM) and dynamic contrast enhanced (DCE) MRI to differentiate benign from malignant breast lesions: A systematic review and meta analysis. *Eur J Radiol.* 2023;167:111051. DOI: 10.1016/j.ejrad.2023.111051.

- 17. Ma W, Mao J, Wang T, Huang Y, Zhao ZH. Distinguishing between benign and malignant breast lesions using diffusion weighted imaging and intravoxel incoherent motion: A systematic review and meta analysis. *Eur J Radiol.* 2021;141:109809. DOI: 10.1016/j.ejrad.2021.109809.
- 18. Liu C, Wang K, Chan Q, Liu Z, Zhang J, He H, et al. Intravoxel incoherent motion MR imaging for breast lesions: comparison and correlation with pharmacokinetic evaluation from dynamic contrast enhanced MR imaging. *Eur Radiol.* 2016;26:3888–98. DOI: 10.1007/s00330-016-4241-6.
- Siemann DW. The unique characteristics of tumor vasculature and preclinical evidence for its selective disruption by tumor vascular disrupting agents. *Cancer Treat Rev.* 2011;37(1):63–74. DOI: 10.1016/j.ctrv.2010.05.001.
- 20. Yuan J, Wong OL, Lo GG, Chan HH, Wong TT, Cheung PS. Statistical assessment of bi exponential diffusion weighted imaging signal characteristics induced by intravoxel incoherent motion in malignant breast tumors. *Quant Imaging Med Surg.* 2016;6(4):418–27. DOI: 10.21037/qims.2016.08.05.
- 21. Panek R, Borri M, Orton M, O'Flynn E, Morgan V, Giles SL, et al. Evaluation of diffusion models in breast cancer. *Med Phys.* 2015;42(8):4833–9. DOI: 10.1118/1.4927255.
- Borlinhas F, Conceição RC, Ferreira HA. Optimal b values for diffusion kurtosis imaging in invasive ductal carcinoma versus ductal carcinoma in situ breast lesions. *Australas Phys Eng Sci Med.* 2019;42:871–85. DOI: https://doi.org/10.1007/s13246-019-00773-2.
- 23. Iima M, Yano K, Kataoka M, Umehana M, Murata K, Kanao S, et al. Quantitative non Gaussian diffusion and intravoxel incoherent motion magnetic resonance imaging: differentiation of malignant and benign breast lesions. *Investig Radiol.* 2015;50(4):205–11. DOI: 10.1097/RLI.0000000000000094.
- 24. Cho GY, Moy L, Kim SG, Baete SH, Moccaldi M, Babb JS, et al. Evaluation of breast cancer using intravoxel incoherent motion (IVIM) histogram analysis: comparison with malignant status, histological subtype, and molecular prognostic factors. *Eur Radiol.* 2016;26:2547–58. DOI: 10.1007/s00330-015-4087-3.
- 25. Perucho JAU, Chang HCC, Vardhanabhuti V, Wang M, Becker AS, Wurnig MC, et al. B value optimization in the estimation of intravoxel incoherent motion parameters in patients with cervical cancer. *Korean J Radiol.* 2020;21(2):218–27. DOI: 10.3348/kjr.2019.0232.
- Chen X, Li WL, Zhang YL, Wu Q, Guo YM, Bai ZL. Meta analysis of quantitative diffusion weighted MR imaging in the differential diagnosis of breast lesions. *BMC Cancer*. 2010;10:134. DOI: 10.1186/1471-2407-10-693.
- Conklin J, Heyn C, Roux M, Cerny M, Wintermark M, Federau C. A simplified model for intravoxel incoherent motion perfusion imaging of the brain. *AJNR Am J Neuroradiol*. 2016;37(12):2251–7. DOI: 10.3174/ajnr.A4929.
- 28. Chen W, Zhang J, Long D, Wang Z, Zhu JM. Optimization of intravoxel incoherent motion measurement in diffusion weighted imaging of breast cancer. *J Appl Clin Med Phys.* 2017;18(3):191–9. DOI: 10.1002/acm2.12065.